Multiple-gap spark gap switch

DOI:
10.1063/1.2216792

Document status and date:
Published: 01/01/2006

Document Version:
Publisher's PDF, also known as Version of Record (includes final page, issue and volume numbers)

Multiple-gap spark gap switch

Z. Liu,[a] K. Yan, G. J. J. Winands, A. J. M. Pemen,
E. J. M. Van Heesch, and D. B. Pawelek
EPS Group, Electrical Department, Technology University of Eindhoven, P.O. Box 513, 5600 MB Eindhoven, The Netherlands

(Received 17 March 2006; accepted 27 May 2006; published online 5 July 2006)

A triggered multiple-gap spark gap switch has been developed and tested under atmosphere. By means of an *LCR* trigger circuit, the multiple-gap switch can be used very reliably. For the same switching voltage (35.5 kV), with increasing the number of gaps from 2 to 6, the switching current rise time is reduced from 13.5 to 6 ns, and the energy efficiency is increased from 87% to 92%. An eight-gap switch was also tested, and the switching current rise time is much smaller than the usable rise time of the current probe (3.5 ns). One interesting application of the multiple-gap switch is to improve the switching performance in the multiple-switch and transmission lines based pulsed power circuit. To verify this application, a six-gap switch was tested. In contrast to a single-gap switch, the output current rise time was improved from 21 to 11 ns by the six-gap switch. © *2006 American Institute of Physics.* [DOI: 10.1063/1.2216792]

I. INTRODUCTION

The spark gap switch has been commonly used in pulsed power system. It can hold a high voltage, carry a large current, and is easy to be constructed. In terms of the number of electrodes, it can be roughly divided into the two/three-electrode switch[1–4] and the multiple-gap (electrodes) switch.[5–7] The advantages of the multiple-gap switch over the two/three-electrode switch are as follows: (a) substantial current cannot flow through the switch until after the last gap has closed; (b) because the last gap is significantly overvolted it closes rapidly; (c) because of the overvoltage the discharge in the multiple gaps works in the multichannel mode;[5,7,8] (d) it is possible to produce a pulse with a fast rise time ($\sim$1 ns) at a high voltage and a low pressure;[8] (e) the short gap distance has a short deionization time,[8] so the multiple gaps switch can be used for the application with a high repetition rate.

In this article, a triggered multiple-gap switch was developed. By means of an *LCR* (inductor-capacitor-resistor) trigger circuit, the multiple-gap switch can be operated very reliably and no external trigger is needed. To study the relationship of the performance of the multiple-gap switch to the number of gaps, two-, four-, six-, and eight-gap switches were tested. One interesting application of the multiple-gap switch is to improve the switching time in the multiple-switch and transmission lines based pulsed power circuit. To verify this application, a six-gap self-breakdown switch was tested in a two-switch setup and compared with a single-gap switch.

II. MULTIPLE-GAP SWITCH WITH AN *LCR* TRIGGER

Figure 1 shows the schematic diagram of the multiple-gap switch experimental setup. It consists of a 1.08 nF high-voltage capacitor C_H, a multiple-gap spark gap switch S, a 50 Ω resistive load, and a trigger circuit. The trigger circuit comprises of an air-core inductor L, a 160 pF capacitor C, and an 80 kΩ resistor R, and we call it *LCR* trigger circuit.[9] The detailed configuration of the experimental setup is shown in Fig. 2. At the left side, the high-voltage capacitor C_H, the switch S, and the load are integrated into a coaxial structure, and at the right side is the *LCR* trigger circuit. As shown in Fig. 2, the switch S was made from seven round aluminum plates. It was designed to hold 36 kV voltage, and the distance of each gap is about 1.5 mm. The middle plate was used as the trigger electrode.

The capacitor C_H was charged by a resonant charging system.[10] During the charging process, the voltages on C_H and on the trigger electrode increase simultaneously. At the end of the charging cycle, the switching voltage is distributed among the six gaps with the averaged electrical field below the breakdown stress of each gap. After the charging is finished, the capacitor C is further charged by the C_H via the *LCR* circuit. The voltage across the gaps between the anode and the trigger electrode increases exponentially ($R \gg \sqrt{L/C}$) until the top three gaps break down. After the trigger gaps close, the gaps between the trigger electrode and the cathode become overvolted, which leads the bottom three gaps to close subsequently.

Figure 3 shows an example of the voltages on C_H and the trigger electrode. The voltage measurements were performed with a Northstar high-voltage probe PVM-1 (ratio 1000:1, bandwidth of 80 MHz). The data were recorded with a LeCroy oscilloscope (wavesurfer 454, 500 MHz, 2 GS/s). The figures in Fig. 3 clearly show the voltage transient during and after the charging process. The voltages on C_H and the trigger electrode increased simultaneously during the charging process, and after the charging is finished the volt-

[a]Electronic mail: z.liu@tue.nl

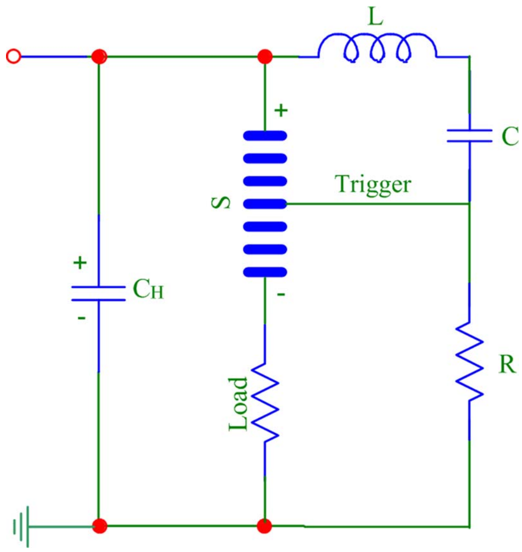

FIG. 1. The schematic diagram of the multiple-gap switch experimental setup.

age on the trigger electrode decreased and the voltage between the anode and the trigger electrode increased until the switch breaks down at 28 μs.

The switching behavior of the multiple-gap switch can be divided into prefiring and normal switching regions. For the normal switching region, the switch always break down after the charging is finished. Figure 4 gives the typical voltage wave forms on C_H for the single shot and the averaged signal from 100 shots. Comparing these two wave forms, one can see that the multiple-gap switch always broke down after the charging is finished, which confirmed that by means of the *LCR* trigger circuit the multiple-gap switch can be used reliably.

The typical output current and voltage are shown in Fig. 5. The current was measured with a Pearson current probe

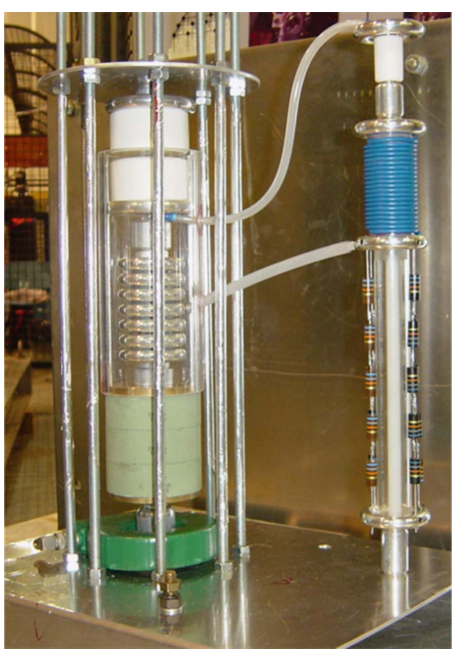

FIG. 2. The photo of the experimental setup.

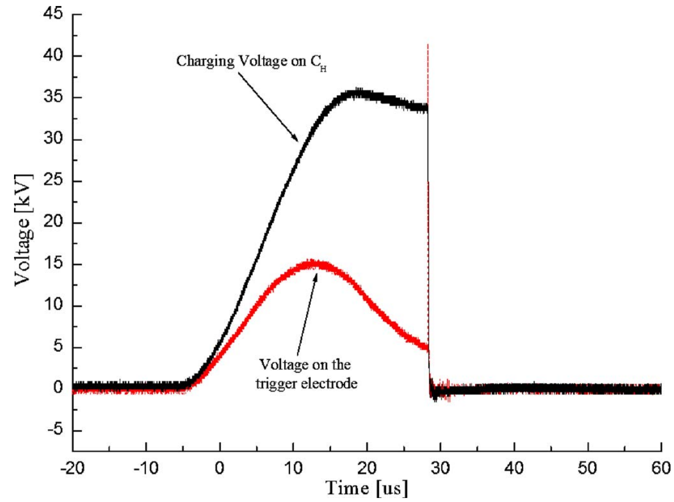

FIG. 3. The typical voltage wave forms on C_H and the trigger electrode.

(model 6600, usable rise time of 3.5 ns). The peak values of the current and the voltage are 595 A and 30.3 kV, respectively. The 10–90% current rise time is about 6 ns.

The energy losses in this circuit are caused by the switch itself and the *LCR* trigger circuit. To evaluate the energy loss caused by the switch itself, the output power P_{out}, the output energy E_{out}, and the energy efficiency η_R were calculated according to the following equations:

$$P_{out} = V_{out} I_{out}, \quad (1)$$

$$E_{out} = \int P_{out} dt, \quad (2)$$

$$\eta_R = E_{out}/E_{total} = E_{out}/0.5 C_H V_b^2. \quad (3)$$

In the above equations, V_{out} is the output voltage on the load and E_{total} and V_b are the energy stored in the capacitor C_H and the voltage on C_H when the switch closes. The typical output power and energy wave forms are shown in Fig. 6. The output peak power and energy are 17.3 MW and 0.558 J, respectively. When the switch closed, the voltage V_b

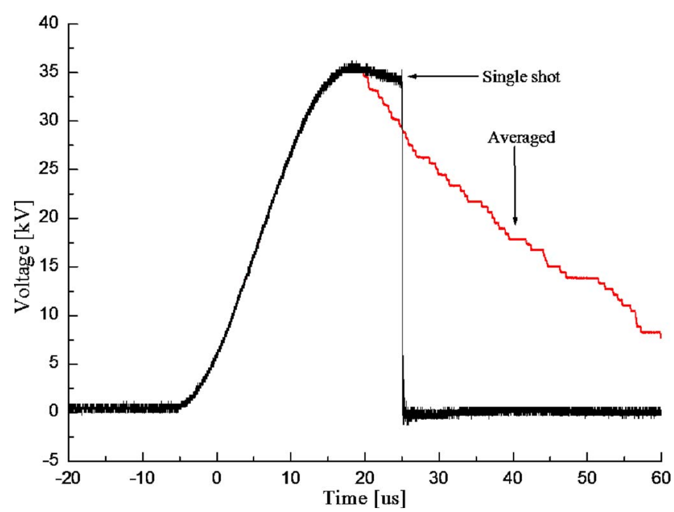

FIG. 4. The typical voltage wave forms on C_H for the single shot and the averaged signal from 100 shots.

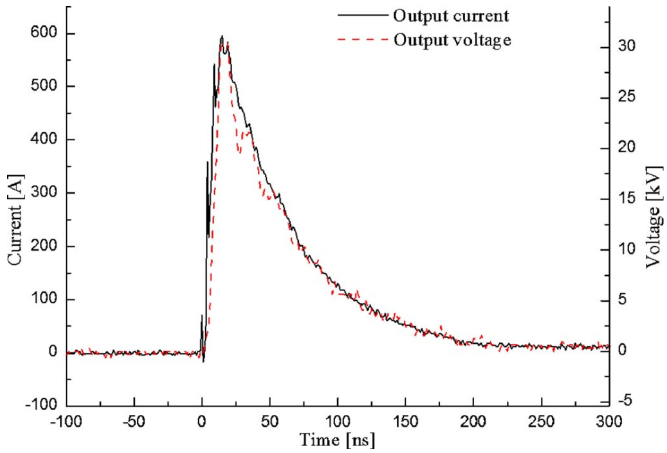

FIG. 5. The typical output current and voltage wave forms.

and the energy E_{total} were 33.5 kV and 0.607 J, respectively. The energy efficiency η_R was 92%. Energy loss caused by the *LCR* trigger circuit was discussed elsewhere.[11]

III. EXPERIMENTAL RESULTS WITH DIFFERENT NUMBER OF THE GAPS

Besides the six-gap spark gap switch, another three switches, i.e., two-, four-, and eight-gap switches, were also constructed and tested. The two-, four-, and eight-gap switches were designed for the same switching voltage with the six-gap switch. The gap distances of the two-, four-, and eight-gap switches are 5.5, 2.5, and 1 mm, respectively. The three switches were tested under the same conditions with the six-gap switch, i.e., the same scale of the setup, the same charging voltage, and the same repetition rate (20 pps) under atmosphere. It was observed that for the eight-gap switch the measured switching current oscillated at the front of the pulse and the rise time was about 1 ns, as shown in Fig. 7. Because the usable rise time of the current probe is 3.5 ns, so the measured switching current for the eight-gap switch cannot be trusted. For the two-, four-, and six-gap switches, no such kind of oscillation occurred.

To study the relationship between the switching performance and the number of gaps, several parameters, such as the total gap distance, the current rise time, the peak output power, and the energy efficiency, were compared. The peak output power and the energy efficiency were calculated by Eqs. (1)–(3). The dependences of these parameters on the number of gaps are shown in Figs. 8 and 9. For all these switches, the C_H was charged up to 35.5 kV. For the two- and four-gap switches, they closed at 34.4 kV, and for the six-gap switch, it closed at 33.5 kV. From Figs. 8 and 9, one can see that with increasing the gap number from 2 to 6, the total gap distance decreases from 11 to 9 mm, and the rise time was improved from 13.5 to 6 ns. The peak output power and the energy efficiency increased from 13.2 to 17.3 MW and from 87.2% to 92%, respectively. Compared with the two- and four-gap switches, though the six-gap switch closed at a lower voltage, its switching current rise time, peak output power, and energy efficiency were improved.

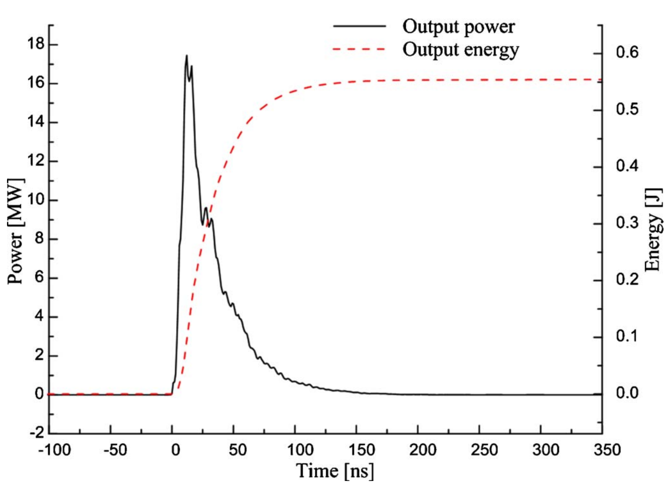

FIG. 6. Typical output power and energy.

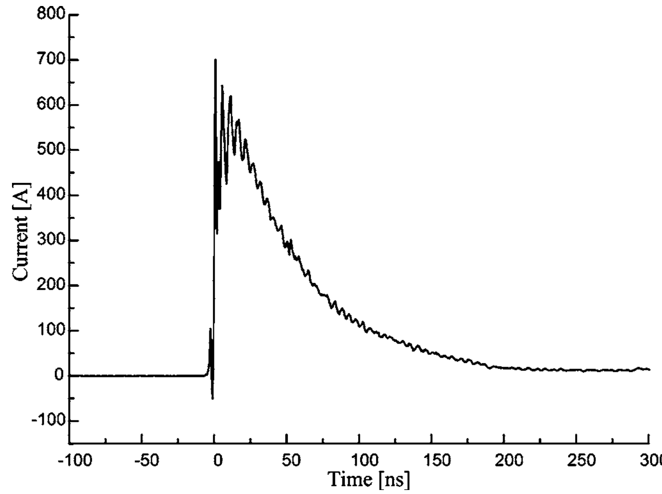

FIG. 7. Typical output current wave form for the eight-gap switch.

IV. TESTING IN THE MULTIPLE-SWITCH BASED PULSED POWER CIRCUIT

An interesting application of the multiple-gap switch is to improve the switching performance in the multiple

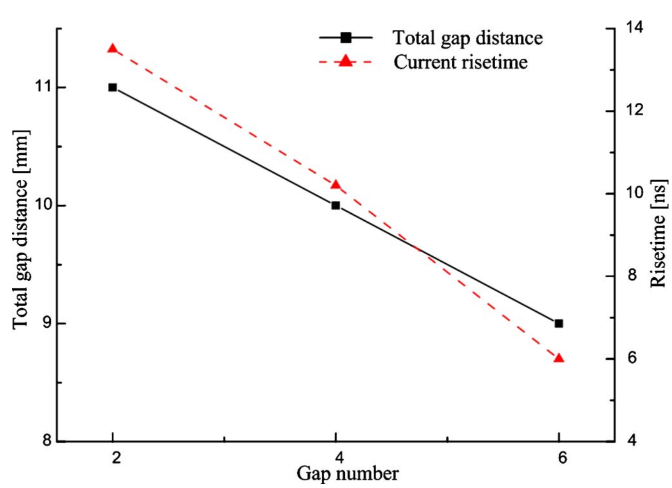

FIG. 8. The dependences of the total gap distance and the current rise time on the number of gaps.

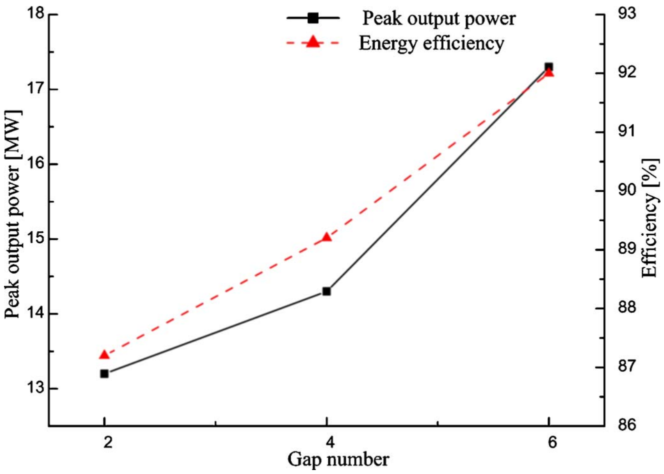

FIG. 9. The dependences of the peak output power and the efficiency on the number of gaps.

switches and transmission lines based pulsed power circuit.[12–14] To verify this application, a two-switch experimental setup was built and tested. The schematic diagram of the two-switch setup is shown in Fig. 10. It includes three inductors L_{1-3}, two 1 nF capacitors C_1 and C_2, two spark gap switches S_1 and S_2, two transmission lines (lines 1 and 2) (RG217), and a 24.4 Ω resistive load. The inductors are used to charge the capacitors C_1 and C_2 in parallel. The C_1 and C_2 are interconnected to the transmission lines (lines 1 and 2) via the switches S_1 and S_2. Magnetic cores are put around lines 1 and 2 to increase the secondary impedance Z_s (the wave impedance between the outsides of the transmission lines). At the output side, the transmission lines are put in parallel and connected to the load.

The unique characteristics of this kind of multiple-switch circuit are (a) the multiple switches can be synchronized by the transmission lines[12,13] and no synchronized trigger circuit is needed; (b) the capacitors C_1 and C_2 cannot discharge rapidly until all the switches are closed, and the switching performance is mainly dominated by the last closed switch.

In this article, the switch S_1 was a triggered spark gap switch and was closed firstly. The switch S_2 was a self-

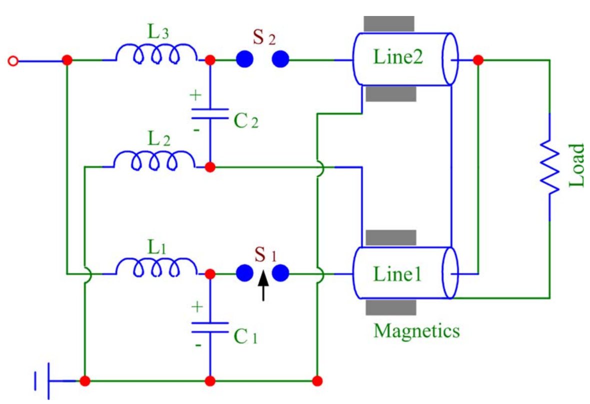

FIG. 10. Schematic diagram of a two-switch pulsed power circuit.

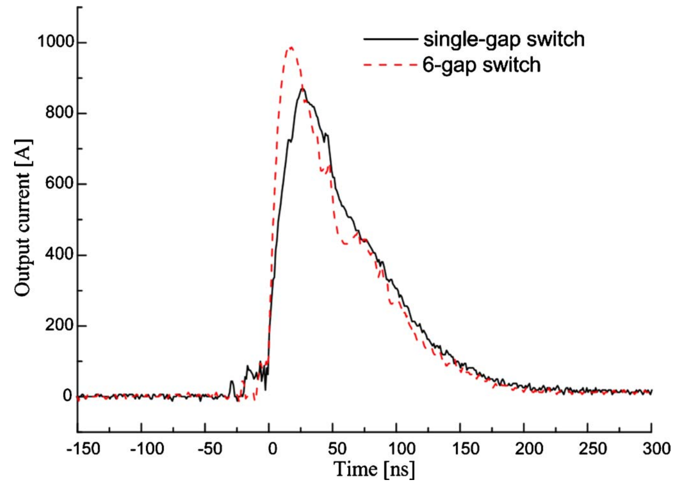

FIG. 11. The output currents when the two different switches were used as S_2.

breakdown spark gap switch and was used as the last closed switch. Two kinds of switches were used as S_2. One is a single-gap spark gap switch with a gap distance of 12.5 mm, the other is a six-gap spark gap switch and each gap distance was 1.5 mm. For both cases, the capacitors C_1 and C_2 were charged up to 33.1 kV, and the switch S_1 was triggered at 32.8 kV and the setup was run at a repetition rate of 10 pps (pulse per second) under atmosphere. Figure 11 gives the typical output currents for both cases. When the single-gap switch was used as S_2, the peak current and the current rise time were 870 A and 21 ns, respectively, while when the six-gap switch was used as S_2, the peak current and current rise time were 993 A and 11 ns, respectively.

[1] J. M. Lehr, C. E. Baum, W. D. Prather, and F. J. Agee, Proceedings of the 11th IEEE Pulsed Power Conference, 1997, pp. 1033—1041.
[2] S. Bower, K. G. Gook, S. Dinsdale, and F. Jones, Proceedings of the 21st Power Modulator Symposium, 1994, pp. 303–305.
[3] J.-L. Parpal, H. P. Mercure, and G. R. Mitchel, IEEE Trans. Electr. Insul. **24**, 1191 (1989).
[4] G. J. J. Winands, Z. Liu, A. J. M. Pemen, E. J. M. Van Heesch, and K. Yan, Rev. Sci. Instrum. **76**, 085107 (2005).
[5] B. M. Kovalchuk, Proceedings of the 11th IEEE Pulsed Power Conference, 1997, pp. 59–67.
[6] B. N. Turman, A. E. Rodriguez, and K. J. Touryan, Proceedings of the Eighth IEEE Pulsed Power Conference, 1991, pp. 319–322.
[7] F. J. Denison *et al.*, Proceedings of the Seventh IEEE Pulsed Power Conference, 1989, pp. 579–582.
[8] G. A. Mesyats, *Pulsed Power* (Kluwer Academic, New York, 2005).
[9] K. Yan, E. J. M. Van Heesch, S. A. Nair, and A. J. M. Pemen, J. Electrost. **57**, 29 (2003).
[10] K. Yan, E. J. M. Van Heesch, A. J. M. Pemen, P. A. H. J. Huijbrechts, and P. C. T. van der Laan, Rev. Sci. Instrum. **72**, 5 (2001).
[11] K. Yan, Ph.D. thesis, Technische Universiteit Eindhoven, 2001; http://alexandria.tue.nl/extra2/200142096.pdf.
[12] K. Yan, H. W. M. Smulders, P. A. A. F. Wouters, S. Kapora, S. A. Nair, E. J. M. Van Heesch, P. C. T. van der Laan, and A. J. M. Pemen, J. Electrost. **58**, 221 (2003).
[13] Z. Liu, K. Yan, A. J. M. Pemen, G. J. J. Winands, and E. J. M. Van Heesch, Rev. Sci. Instrum. **76**, 113507 (2005).
[14] K. Yan, E. J. M. Van Heesch, P. A. A. F. Wouters, A. J. M. Pemen, and S. A. Nair, 2002 Power Modulator Symposium and 2002 High-Voltage Workshop, Conference Record of the 25th International, 30 June–3 July 2002, pp. 420–423.